


Linear response functions respecting Ward-Takahashi identity and fluctuation-dissipation theorem within the *GW* approximation

Hui Li ¹, Zhipeng Sun ^{2,*}, Yingze Su ¹, Haiqing Lin ^{2,†}, Huaqing Huang ^{1,‡} and Dingping Li ^{1,§}

¹*School of Physics, Peking University, Beijing 100871, China*

²*Beijing Computational Science Research Center, Beijing 100193, China*

 (Received 22 August 2022; revised 4 December 2022; accepted 18 January 2023; published 6 February 2023)

Fundamental equalities, such as the Ward-Takahashi identity (WTI) and the fluctuation-dissipation theorem (FDT), are important in the calculation of the response functions, which are defined as the variations of physical quantities with respect to the external sources. In this paper, the formalism of calculating the response functions according to their original definitions is presented, based on the generalized *GW* (GGW) method which was developed for the electronic systems including spin-dependent interaction. This formalism automatically ensures the FDT, and is theoretically proved to respect the WTI. By contrast, the commonly used random phase approximation (RPA) within the GGW method violates both the WTI and the FDT, and the Bethe-Salpeter equation (BSE) satisfies the WTI but does not fulfill the FDT. The validity of this methodology is demonstrated on the two-dimensional one-band Hubbard model, and the results show that our formalism makes significant improvements over the RPA formula. Due to the similar computational cost to the BSE, our formalism is expected to be applied to realistic materials.

DOI: [10.1103/PhysRevB.107.085106](https://doi.org/10.1103/PhysRevB.107.085106)

I. INTRODUCTION

Response functions, such as the spin susceptibility, the charge compressibility and the electronic conductivity, are important quantities to describe the physical properties of realistic materials. The numerical computation of the response functions has always been a central issue in condensed matter physics, which directly relates to the experimental results [1]. Even for a given many-body model, such as the Hubbard model, the existing theoretical framework cannot provide an accurate and strict calculation. Approximations are necessary to be introduced, and thus the accuracy of the calculation is concerning. Also, respecting the fundamental equalities is also particularly important. Baym and Kadanoff [2] pointed out the importance of the charge conservation for many-body systems, and proposed a scheme to ensure the Ward-Takahashi identity (WTI). However, the commonly used random phase approximation (RPA) and Bethe-Salpeter equation (BSE) within the *GW* framework in realistic materials do not strictly follow the Baym-Kadanoff framework [3]. Therefore, their deviation from the fundamental equalities is worrying and worth studying. As shown in Ref. [4], the deviation of the WTI is negatively related to the quality of the calculation accuracy within the *GW* framework. In Ref. [5], it is pointed out that the charge compressibility is larger by about three times than the value given by the renormalized RPA within the fluctuation-exchange approx-

imation, which is exactly the consequence of violating the fluctuation-dissipation theorem (FDT). It can be said that it is very important to ensure the fundamental equalities in the calculation of the response functions.

It should be pointed out that the physical response functions are defined as the variations of the physical quantities with respect to the external sources, and are functional derivatives in the mathematical forms. This definition automatically satisfies the FDT, so as to guarantee the Kubo's formula [6]: the bridge between the response functions and the correlation functions. For this reason, the response functions should be calculated from their own definitions, i.e., the functional derivatives, and such an idea began with Ornstein and Zernike [7]. Such an idea is also applied to the mean-field analysis of the Ising model in the statistical mechanics, where the physical spin susceptibility is calculated by the functional derivative of the mean local spin with respect to the external magnetic field (for example in Ref. [8]). In quantum field theory, the propagator calculated by the functional derivative can restore the important Goldstone theorem and higher-order WTIs [9–11]. Therefore, in the realistic materials, we believe it is also important to calculate the response functions from their original definitions.

In this paper, we study the scheme of calculating the response functions according to their definitions, based on the existing generalized *GW* (GGW) approximation [12–19], which was developed for the systems including the spin-dependent interaction. We theoretically proved that the functional derivative scheme preserves the WTI, as is required for a self-consistent method. We calculated the deviations of the RPA, the BSE and the functional derivative scheme approaches from the WTI and FDT in the two-dimensional Hubbard model. The results show that the RPA has an obvious

*zpsun@csrc.ac.cn

†haiqing0@csrc.ac.cn

‡huanghq07@pku.edu.cn

§lidp@pku.edu.cn

deviation from both the WTI and the FDT; the BSE satisfies the WTI whereas violates the FDT; the functional derivative respect both of them, as proved theoretically. We also made some numerical comparisons with the results obtained with the determinantal quantum Monte Carlo (DQMC) and dynamical mean field theory (DMFT). The results show that the functional derivative scheme makes a significant improvement over the RPA, and competes with the DMFT within the range of parameters considered. Noting that the functional derivative scheme has a similar computation complexity to the BSE, it could also be applied to some realistic materials.

The paper is organized as follows. In Sec. II we present the formalism of the GW approximation for general electronic systems, and apply the functional derivative scheme to the GW approximation. Next in Sec. III, we apply our method to the two-dimensional Hubbard model. In Sec. IV, we present the numerical results of our approach. The conclusion is given in Sec. V.

II. FORMALISM

A. GW approximation in general cases

The generalized GW approximation was proposed to deal with explicitly spin-dependent interaction, and can be applied to various kinds of electronic systems. We reformulate it in the functional path integral formalism, and start with the Matsubara action:

$$S[\psi^*, \psi] = - \sum_{\alpha_1 \alpha_2} \int d(12) \psi_{\alpha_1}^*(1) T_{\alpha_1 \alpha_2}(1, 2) \psi_{\alpha_2}(2) + \frac{1}{2} \int d(12) \sum_{ab} \sigma^a(1) V^{ab}(1, 2) \sigma^b(2). \quad (1)$$

Here, the charge/spin composite operator $\sigma^a(1) = \sum_{\alpha\alpha'} \psi_{\alpha}^*(1) \tau_{\alpha\alpha'}^a \psi_{\alpha'}(1)$, $\tau^a (a = 0, x, y, z)$ are Pauli matrices, Greek letters like α indicate spin up and spin down. ψ, ψ^* are Grassmannian fields. Notation $(1) = (\tau_1, \vec{x}_1)$ contains the space coordinate x_1 , and the imaginary time coordinate $0 \leq \tau_1 \leq \beta$, where β is the inverse temperature. The notation $\int d(1)$ stands for integral over all space and time coordinates in the continuous system, and stands for the summation over all space and time coordinates in the discrete system. The two-body interaction is symmetric, i.e., $V^{ab}(1, 2) = V^{ba}(2, 1)$, and it can describe the usual Coulomb interaction, the spin-spin interaction, and the spin-orbit interaction.

The one-body Green's function is defined in an ensemble average form:

$$G_{\alpha_1 \alpha_2}(1, 2) = \langle \psi_{\alpha_2}^*(2) \psi_{\alpha_1}(1) \rangle. \quad (2)$$

$\langle \dots \rangle$ presents for $\frac{1}{Z} \int D[\psi^*, \psi] \dots e^{-S}$, with $Z = \int D[\psi^*, \psi] e^{-S}$ the grand partition function, and $D[\psi^*, \psi] = \prod_n d(\psi_n^*, \psi_n)$ defines the measure (for each field index n we have an integration over a coherent state basis) [20]. Since the interaction has a spin structure, it is convenient to denote the matrix in the spin space as

$$\underline{X} = \begin{bmatrix} X_{\uparrow\uparrow} & X_{\uparrow\downarrow} \\ X_{\downarrow\uparrow} & X_{\downarrow\downarrow} \end{bmatrix}. \quad (3)$$

Note that its trace is denoted by $\text{Tr}[\underline{X}] = X_{\uparrow\uparrow} + X_{\downarrow\downarrow}$.

Then one can derive the generalized Hedin's equations for the action Eq. (1), and the lowest approximation for the Hedin's vertex function leads to the GW approximation. The full Green's function, \underline{G} , is determined from the bare Green's function \underline{T} and self-energy, through Dyson's equation: $\underline{G}^{-1}(1, 2) = \underline{T}(1, 2) - \underline{\Sigma}_H - \underline{\Sigma}(1, 2)$. In the GW approximation, the Hartree self-energy is given by

$$\underline{\Sigma}_H(1, 2) = \delta(1, 2) \sum_{ab} \int d(4) \underline{\tau}^a V^{ab}(1, 4) \text{Tr}[\underline{\tau}^b \underline{G}(4, 4)], \quad (4)$$

and the GW self-energy is given by

$$\underline{\Sigma}(1, 2) = - \sum_{ab} \underline{\tau}^a \underline{G}(1, 2) \underline{\tau}^b W^{ba}(2, 1), \quad (5)$$

where W is the dynamic effective charge/spin potential and determined by the polarization function P through the relation $(W^{-1})^{ab}(1, 2) = (V^{-1})^{ab}(1, 2) - P^{ab}(1, 2)$. The polarization function is approximated by

$$P^{ab}(1, 2) = \text{Tr}[\underline{\tau}^a \underline{G}(1, 2) \underline{\tau}^b \underline{G}(2, 1)]. \quad (6)$$

These equations can be solved self-consistently. It is worth mentioning that, in the GW approximation, the Green's function \underline{G} and the self-energy $\underline{\Sigma}$ are spin-dependent, the screened potential W and the polarization function P are 4×4 matrices containing the coherence between charge and spin channels. Next, we will address the problem of the two-body correlation functions.

B. Covariant scheme for the GW method

For the generalized Hartree (GH) approximation, which only contains Hartree self-energy in Eq. (4), the two-body correlation function obtained by RPA formula can preserve the FDT and WTI (the vertex at the two-body level only contains the first two diagrams in Fig. 1). However, the higher-order approximation, such as GW, cannot preserve both the FDT and the WTI when using the RPA formula to calculate the two-body correlation. Therefore, in this subsection, we take the GW approximation as an example to derive the physical response function calculation for the higher-order approximation theory.

According to the FDT, the two-body correlation functions should be defined as the response of the physical quantity in the presence of an external potential, which we refer to as the covariant scheme. The scheme for calculating a general connected two-body correlation function $\chi_{XY}(1, 2) = \langle X(1)Y(2) \rangle_c$ within the GW framework, where X, Y are binary composite operators, is formulated as follows.

First, one adds the corresponding source term to the action, $S[\psi^*, \psi; \phi] = S[\psi^*, \psi] - \int d(1) \phi(1) X(1)$ and the correlation can be obtained by $\chi_{XY}(1, 2) = \frac{\delta \langle Y(2) \rangle}{\delta \phi(1)}$. Then, we write down the off-shell GW equations (keep $\phi \neq 0$), and calculate the functional derivative of the GW equations with respect to ϕ . Finally, let the source ϕ tend to 0 to obtain the on-shell results. Although we restrict our discussion to the GW, this scheme can also be applied to different many body approaches.

We consider the calculation of a general connected two-body correlation function $\chi_{XY}(1, 2) = \langle X(1)Y(2) \rangle -$

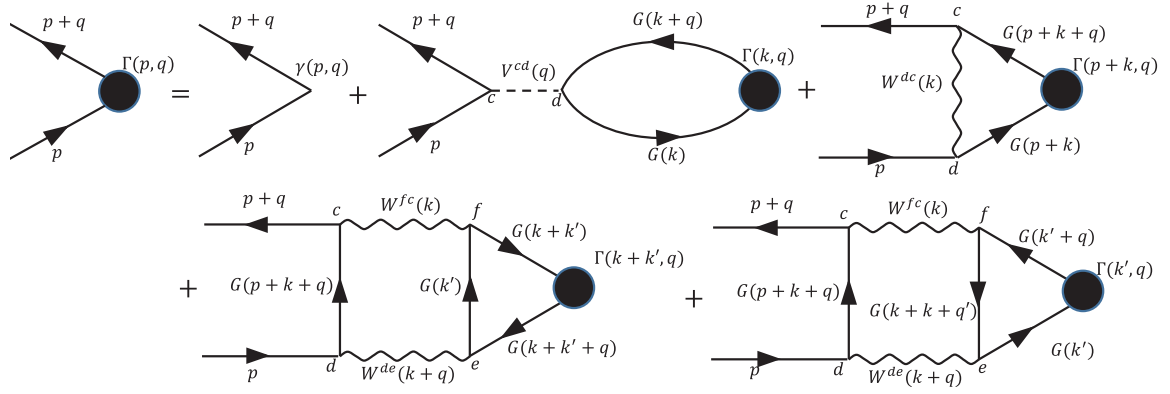


FIG. 1. The Feynman diagram of the full cGGW vertex function in Eq. (12) for translation invariant systems in the momentum space.

$\langle X(1) \rangle \langle Y(2) \rangle$, where X, Y are local binary operators and take the form

$$X(1) = \sum_{\alpha_2 \alpha_3} \int d(23) \psi_{\alpha_2}^*(2) K_{X; \alpha_2 \alpha_3}(1, 2, 3) \psi_{\alpha_3}(3). \quad (7)$$

The expression for the kernel K depends on the operator X . As for the spin operator, the kernel K for $\sigma^a(1) = \sum_{\alpha_1 \alpha'_1} \psi_{\alpha_1}^*(1) \tau_{\alpha_1 \alpha'_1}^a \psi_{\alpha'_1}(1)$ is

$$K_{\sigma^a; \alpha_2, \alpha_3}(1, 2, 3) = \delta(1, 2) \delta(1, 3) \tau_{\alpha_2 \alpha_3}^a. \quad (8)$$

First, we add an external local source $\phi(1)$ coupled to the operator $X(1)$ and thus the perturbed action becomes

$$S[\psi^*, \psi, \phi] = S[\psi^*, \psi] - \int d(1) \phi(1) X(1). \quad (9)$$

The additional term $\int d(1) \phi(1) X(1)$ is explicitly expressed as

$$\int d(123) \sum_{\alpha_1 \alpha_2} \psi_{\alpha_1}^*(1) \{ \phi(3) K_{X; \alpha_1 \alpha_2}(3, 1, 2) \} \psi_{\alpha_2}(2). \quad (10)$$

Note that the additional term can be regarded as a variation of the T term:

$$\underline{T}(1, 2; \phi) = \underline{T}(1, 2) + \int d(3) \phi(3) \underline{K}_X(3, 1, 2). \quad (11)$$

The functional derivative of the off-shell GGW equations with respect to the external source ϕ leads to the covariant GGW (cGGW) equations. The equation involves the full vertex function $\underline{\Gamma}_\phi(1, 2, 3) = \frac{\delta \underline{G}^{-1}(1, 2)}{\delta \phi(3)}$, which consists of five terms shown in Fig. 1:

$$\begin{aligned} \underline{\Gamma}_\phi(1, 2, 3) = & \underline{\gamma}_\phi(1, 2, 3) + \underline{\Gamma}_{\phi, H}(1, 2, 3) + \underline{\Gamma}_{\phi, MT}(1, 2, 3) \\ & + \underline{\Gamma}_{\phi, AL1}(1, 2, 3) + \underline{\Gamma}_{\phi, AL2}(1, 2, 3). \end{aligned} \quad (12)$$

Here, the bare vertex $\underline{\gamma}_\phi$ depends on the operator X , is calculated through

$$\underline{\gamma}_\phi(1, 2, 3) \equiv \frac{\delta \underline{T}(1, 2; \phi)}{\delta \phi(3)} = \underline{K}_X(3, 1, 2). \quad (13)$$

In the charge/spin response case, $X^a = \sigma^a$, the bare vertex takes the form $\underline{\gamma}_\phi(1, 2, 3) = \tau^a \delta(1, 2) \delta(1, 3)$. The ‘‘bubble’’ vertex is induced by the Hartree self-energy, i.e., $\underline{\Gamma}_{\phi, H} = -\delta \Sigma_H / \delta \phi$, and takes the form

$$\underline{\Gamma}_{\phi, H}(1, 2, 3) = -\delta(1, 2) \sum_{cd} \int d(456) \tau^c V^{cd}(1, 4) \text{Tr}[\tau^d \underline{G}(1, 5) \underline{\Gamma}_\phi(5, 6, 3) \underline{G}(6, 2)]. \quad (14)$$

Note that the conventional RPA-like formula only consists of the first two terms in Eq. (12). The Maki-Thompson-like (MT) vertex and two distinct Aslamazov-Larkin-like (AL) vertices [21] are induced by the self-energy, i.e., $\underline{\Gamma}_\phi = -\delta \Sigma / \delta \phi$, representing the vertex corrections beyond the RPA, and take the form

$$\underline{\Gamma}_{\phi, MT}(1, 2, 3) = -\sum_{cd} \int d(45) \underline{\tau}^c \underline{G}(1, 4) \underline{\Gamma}_\phi(4, 5, 3) \underline{G}(5, 2) \underline{\tau}^d W^{dc}(2, 1), \quad (15)$$

$$\underline{\Gamma}_{\phi, AL1}(1, 2, 3) = -\sum_{cdef} \int d(4567) \underline{\tau}^c \underline{G}(1, 2) \underline{\tau}^d W^{de}(1, 4) W^{fc}(5, 2) \text{Tr}[\underline{\tau}^e \underline{G}(4, 6) \underline{\Gamma}_\phi(6, 7, 3) \underline{G}(7, 5) \underline{\tau}^f \underline{G}(5, 4)], \quad (16)$$

$$\underline{\Gamma}_{\phi, AL2}(1, 2, 3) = -\sum_{cdef} \int d(4567) \underline{\tau}^c \underline{G}(1, 2) \underline{\tau}^d W^{de}(1, 4) W^{fc}(5, 2) \text{Tr}[\underline{\tau}^e \underline{G}(4, 5) \underline{\tau}^f \underline{G}(5, 6) \underline{\Gamma}_\phi(6, 7, 3) \underline{G}(7, 4)]. \quad (17)$$

Finally, let $\phi \rightarrow 0$ and solve the self-consistent Eqs. (12)–(17) to obtain the full vertex function $\underline{\Gamma}_\phi$.

Since the average $\langle Y(2) \rangle$ is a function of the Green's function G , the two-body correlation function $\chi_{XY}(1, 2)$ can be obtained by the vertex $\underline{\Gamma}_\phi$:

$$\langle X(1)Y(2) \rangle_c \equiv \frac{\delta \langle Y(2) \rangle}{\delta \phi(1)} = \int d(34) \text{Tr} \left[\underline{K}_Y(2, 3, 4) \frac{\delta \underline{G}(4, 3)}{\delta \phi(1)} \right] = - \int d(3456) \text{Tr} [\underline{K}_Y(2, 3, 4) \underline{G}(4, 5) \underline{\Gamma}_\phi(5, 6, 1) \underline{G}(6, 3)]. \quad (18)$$

For example, when calculating the spin-spin correlation $\chi_s^{ab}(1, 2) = \langle \sigma^a(1) \sigma^b(2) \rangle$, the above equation can be simplified as

$$\chi_s^{ab}(1, 2) = - \int d(56) \text{Tr} [\underline{\tau}^b \underline{G}(2, 5) \underline{\Gamma}_\phi(5, 6, 1) \underline{G}(6, 2)]. \quad (19)$$

Such response functions satisfy the FDT by definition, and the preserving of the WTI is proven in the next subsection.

C. Ward-Takahashi identity

Notice that there is the charge $U(1)$ symmetry in the system, thus we consider the $U(1)$ WTI here. Without loss of generality, the discussion and the proof are based on the continuous system and the T - term in the Eq (1) takes the following form:

$$\underline{T}(1, 2) = \delta(1, 2) \left[-\partial_{\tau_2} + \frac{\nabla_{\vec{x}_2}^2}{2m} - \mu \right] \underline{\tau}^0. \quad (20)$$

Here m is the mass of the electron and $\nabla_{\vec{x}_2}^2$ is the Laplace operator acting on the coordinate \vec{x}_2 . Due to the global charge $U(1)$ symmetry, one can obtain the lowest order WTI, i.e., the well-known charge current conservation equation,

$$\frac{\partial \langle \rho(1) \rangle}{\partial \tau} - \sum_\nu \partial_\nu \langle j^\nu(1) \rangle = 0, \quad (21)$$

where $\rho(1) = \sum_\alpha \psi_\alpha^*(1) \psi_\alpha(1)$ is the charge density, $\nu = x, y, z, \dots$ is the direction of the current. The current operator is given by [22,23]

$$\begin{aligned} j^\nu(1) &= \frac{1}{2m} \sum_\alpha [\psi_\alpha^*(1) \partial_\nu \psi_\alpha(1) + \psi_\alpha(1) \partial_\nu \psi_\alpha^*(1)] \\ &\triangleq \frac{1}{2m} \sum_\alpha \psi_\alpha^*(1) (\overrightarrow{\partial}_\nu - \overleftarrow{\partial}_\nu) \psi_\alpha(1), \end{aligned} \quad (22)$$

where $\overrightarrow{\partial}_\nu$ acting on the right function and $\overleftarrow{\partial}_\nu$ acting on the left. This lowest order WTI can be directly verified by rewritten in the form (for the derivation of the WTI, see Appendix A 1):

$$\int d(2) \text{Tr} [\underline{T}(1, 2) \underline{G}(2, 1)] = \int d(2) \text{Tr} [\underline{T}(2, 1) \underline{G}(1, 2)]. \quad (23)$$

One can also derive the high-order WTI based on the $U(1)$ gauge symmetry:

$$\begin{aligned} &\langle \partial_\mu j^\mu(1) \psi_{\alpha_2}^*(2) \psi_{\alpha_3}(3) \rangle - \langle \partial_\tau \rho(1) \psi_{\alpha_2}^*(2) \psi_{\alpha_3}(3) \rangle \\ &= -\delta(1, 2) \delta_{\alpha_1 \alpha_2} G_{\alpha_3 \alpha_2}(3, 2) + \delta(1, 3) \delta_{\alpha_1 \alpha_3} G_{\alpha_3 \alpha_2}(3, 2). \end{aligned} \quad (24)$$

Such a WTI relates the current correlation function to the Green's function, representing the charge current conservation on the two-body correlation level. This WTI can be written in terms of the current vertex and the density vertex functions:

$$\begin{aligned} &\sum_{\nu_3} \partial_{\nu_3} \underline{\Gamma}^{\nu_3}(1, 2, 3) - \partial_{\tau_3} \underline{\Gamma}^\rho(1, 2, 3) \\ &= \delta(3, 1) \underline{G}^{-1}(3, 2) - \delta(3, 2) \underline{G}^{-1}(1, 3). \end{aligned} \quad (25)$$

Here the vertex corresponding to the current j^ν is defined as

$$\begin{aligned} \Gamma_{\alpha_1 \alpha_2}^{\nu_3}(1, 2, 3) &= - \int d(45) \sum_{\alpha_4 \alpha_5} G_{\alpha_1 \alpha_4}^{-1}(1, 4) \\ &\quad \times \langle \psi_{\alpha_5}^*(5) \psi_{\alpha_4}(4) j^{\nu_3}(3) \rangle G_{\alpha_5 \alpha_2}^{-1}(5, 2), \end{aligned} \quad (26)$$

and the vertex corresponding to the density operator ρ is defined as

$$\begin{aligned} \Gamma_{\alpha_1 \alpha_2}^\rho(1, 2, 3) &= - \int d(45) \sum_{\alpha_4 \alpha_5} G_{\alpha_1 \alpha_4}^{-1}(1, 4) \\ &\quad \times \langle \psi_{\alpha_5}^*(5) \psi_{\alpha_4}(4) \rho(3) \rangle G_{\alpha_5 \alpha_2}^{-1}(5, 2). \end{aligned} \quad (27)$$

Then we will prove the vertex Eq. (12) in the cGGW method is compatible with the WTI (25) below. The bare vertices in the cGGW equations can be obtained through the current operator kernel $\underline{K}_{j^\nu}(1, 2, 3) = \delta(1, 2) \delta(1, 3) (\overrightarrow{\partial}_{\nu_1} - \overleftarrow{\partial}_{\nu_1}) \underline{\tau}^0 / 2m$ and the density operator kernel $\underline{K}_\rho(1, 2, 3) = \delta(1, 2) \delta(1, 3) \underline{\tau}^0$:

$$\underline{\gamma}^{\nu_3}(1, 2, 3) = \delta(1, 2) \delta(1, 3) \frac{1}{2m} [\overrightarrow{\partial}_{\nu_3} - \overleftarrow{\partial}_{\nu_3}] \underline{\tau}^0, \quad (28)$$

$$\underline{\gamma}^\rho(1, 2, 3) = \delta(1, 2) \delta(1, 3) \underline{\tau}^0, \quad (29)$$

and the corresponding cGGW vertex is determined by Eqs. (12)–(17).

We start the proof from the right-hand side of Eq. (25), i.e., $\delta(3, 1) \underline{G}^{-1}(3, 2) - \delta(3, 2) \underline{G}^{-1}(1, 3)$. By virtue of the Dyson's equation, it can be rewritten as

$$\begin{aligned} &[\delta(3, 1) \underline{T}(3, 2) - \delta(3, 2) \underline{T}(1, 3)] \\ &+ [-\delta(3, 1) \underline{\Sigma}(3, 2) + \delta(3, 2) \underline{\Sigma}(1, 3)]. \end{aligned} \quad (30)$$

The first term in Eq. (30) can be rewritten in form of the bare vertices directly:

$$\sum_{\nu_3} \partial_{\nu_3} \underline{\gamma}^{\nu_3}(1, 2, 3) - \partial_{\tau_3} \underline{\gamma}^\rho(1, 2, 3) \triangleq \Gamma_1^{\text{WTI}}(1, 2, 3). \quad (31)$$

By virtue of Eq. (5), the second term in Eq. (30) can be rewritten as

$$-\sum_{cd} \int d(45) \underline{\tau}^c \underline{G}(1, 4) [\delta(3, 4) \underline{G}^{-1}(3, 5) - \delta(3, 5) \underline{G}^{-1}(4, 3)] \underline{G}(5, 2) \underline{\tau}^d W^{dc}(2, 1). \quad (32)$$

Then substituting the WTI (25) into Eq. (32), one obtains

$$-\sum_{cd} \int d(45) \underline{\tau}^c \underline{G}(1, 4) \left[\sum_{\nu_3} \partial_{\nu_3} \underline{\Gamma}^{\nu_3}(4, 5, 3) - \partial_{\tau_3} \underline{\Gamma}^{\rho}(4, 5, 3) \right] \underline{G}(5, 2) \underline{\tau}^d W^{dc}(2, 1) \triangleq \Gamma_2^{\text{WTI}}(1, 2, 3). \quad (33)$$

Then one concludes the right-hand side of Eq. (25) equals to $\Gamma_1^{\text{WTI}}(1, 2, 3) + \Gamma_2^{\text{WTI}}(1, 2, 3)$. Now we substitute the cGGW vertex Eq. (12) into the left-hand side of Eq. (25), and obtain

$$\begin{aligned} & \sum_{\nu_3} \partial_{\nu_3} \underline{\Gamma}^{\nu_3}(1, 2, 3) - \partial_{\tau_3} \underline{\Gamma}^{\rho}(1, 2, 3) \\ &= \sum_{\nu_3} \partial_{\nu_3} \underline{\gamma}^{\nu_3}(1, 2, 3) - \partial_{\tau_3} \underline{\gamma}^{\rho}(1, 2, 3) + \sum_{\nu_3} \partial_{\nu_3} \underline{\Gamma}_{\text{H}}^{\nu_3}(1, 2, 3) - \partial_{\tau_3} \underline{\Gamma}_{\text{H}}^{\rho}(1, 2, 3) + \sum_{\nu_3} \partial_{\nu_3} \underline{\Gamma}_{\text{MT}}^{\nu_3}(1, 2, 3) - \partial_{\tau_3} \underline{\Gamma}_{\text{MT}}^{\rho}(1, 2, 3) \\ &+ \sum_{\nu_3} \partial_{\nu_3} \underline{\Gamma}_{\text{AL1}}^{\nu_3}(1, 2, 3) - \partial_{\tau_3} \underline{\Gamma}_{\text{AL1}}^{\rho}(1, 2, 3) + \sum_{\nu_3} \partial_{\nu_3} \underline{\Gamma}_{\text{AL2}}^{\nu_3}(1, 2, 3) - \partial_{\tau_3} \underline{\Gamma}_{\text{AL2}}^{\rho}(1, 2, 3). \end{aligned} \quad (34)$$

The first term in the right-hand side of Eq. (34) equals to $\Gamma_1^{\text{WTI}}(1, 2, 3)$, and the third term equals to $\Gamma_2^{\text{WTI}}(1, 2, 3)$. In Appendix A 2, we show the second term is zero, and the sum of the fourth and fifth terms is also zero. Therefore, the compatibility of the WTI and the vertex equation is proved. Although we prove the cGGW vertex satisfies the $U(1)$ WTI for the continuous system, such proof can be extended to the lattice system, which will be shown in the two-dimensional Hubbard model.

Note that, in the BSE approach, the two AL vertices in Eq. (12) are ignored. Therefore, the BSE approach also preserves the WTI, however, violates the FDT.

III. IMPLEMENTATION IN THE TWO-DIMENSIONAL HUBBARD MODEL

A. Matsubara action in the discretized time path integral formalism

The Hamiltonian of the Hubbard model is

$$\hat{H} = -t \sum_{\langle ij \rangle} \sum_{\alpha=\uparrow, \downarrow} \hat{\psi}_{i\alpha}^\dagger \hat{\psi}_{j\alpha} + U \sum_i \hat{n}_{i\uparrow} \hat{n}_{i\downarrow} - \mu \sum_{i\sigma} \hat{n}_{i\sigma}, \quad (35)$$

where $\hat{\psi}_{\vec{x}_1\alpha}^\dagger$ creates an electron with spin α at lattice site \vec{x}_1 and $\hat{n}_{i\sigma} = \hat{\psi}_{i\sigma}^\dagger \hat{\psi}_{i\sigma}$ denotes the spin-resolved density operator. t is the (nearest-neighbor) hopping amplitude and all energies are given in units of $t = 1$ in this paper. $\langle \vec{x}_1 \vec{x}_2 \rangle$ denotes summation over nearest-neighbor lattice sites, U is the on-site interaction, and μ is the chemical potential. The widely used GW approximation for the Hubbard model is based on the Hamiltonian Eq. (35) and denoted by GW in the following.

One should notice that the intrinsic symmetries of the Hubbard are not only global charge $U(1)$ but also spin $SU(2)$, where the latter one constrains the spin-spin correlation satisfying $\chi_{sp}^{xx} = \chi_{sp}^{yy} = \chi_{sp}^{zz}$ in the paramagnetic phase. However, we find the spin-spin correlation function obtained by the traditional GW in the different directions is not equal to each other. (The traditional GW equations and related results are shown in Appendix C).

To preserve the spin $SU(2)$ symmetry, we rewrite the Hubbard Hamiltonian as [24]

$$\begin{aligned} \mathcal{H} &= -t \sum_{\langle \vec{x}_1 \vec{x}_2 \rangle \alpha} \psi_{\vec{x}_1\alpha}^\dagger \psi_{\vec{x}_2\alpha} - \frac{U}{6} \sum_{\vec{x}} \sum_{a=x,y,z} \sigma_{\vec{x}}^a \sigma_{\vec{x}}^a \\ &- \left(\mu - \frac{U}{2} \right) \sum_{\alpha\bar{\alpha}} \psi_{\alpha\bar{\alpha}}^\dagger \psi_{\alpha\bar{\alpha}}. \end{aligned} \quad (36)$$

Here we use the relation

$$U \hat{n}_{i\uparrow} \hat{n}_{i\downarrow} = \frac{I_s}{2} \sum_{a=x,y,z} \hat{\sigma}_i^a \hat{\sigma}_i^a + \frac{U}{2} \sum_{i\alpha} \hat{n}_{i\alpha}, \quad (37)$$

where $I_s = -\frac{U}{3}$.

We use the discretized Matsubara time path integral formalism [25] for the numerical implementation. The discretized-time action for the Hubbard Hamiltonian reads

$$\begin{aligned} S_M[\psi^*, \psi] &= \sum_{l=0}^{M-1} \sum_{\alpha=\uparrow, \downarrow} \sum_{\vec{x}} \{ \psi_\alpha^*(\vec{x}, \tau_l) (\psi_\alpha(\vec{x}, \tau_{l+1}) - \psi_\alpha(\vec{x}, \tau_l)) \} \\ &+ \sum_{l=1}^{M-1} \Delta\tau \mathcal{H}[\psi_\alpha^*(\vec{x}, \tau_l) \psi_\alpha(\vec{x}, \tau_l)]. \end{aligned} \quad (38)$$

Here M is the number of time slices, and $\Delta\tau = \beta/M$. The integer l labels the discretized Matsubara time, and $\tau_l \equiv l\Delta\tau$.

Compare the action (38) with the form (1), and one obtains

$$\begin{aligned} \underline{T}(1, 2) &= \left[-\frac{1}{\Delta\tau} \delta_{\vec{x}_1 \vec{x}_2} (\delta_{l_1, l_2-1} - \delta_{l_1, l_2}) + t_{\vec{x}_1 \vec{x}_2} \delta_{l_1, l_2} + \mu \delta_{\vec{x}_1 \vec{x}_2} \delta_{l_1, l_2} \right] \underline{\tau}^0, \end{aligned} \quad (39)$$

and

$$V^{ab}(1, 2) = \delta_{\vec{x}_1 \vec{x}_2} \delta_{l_1 l_2} \delta^{ab} I_s, \quad (40)$$

with a, b taking values of x, y, z . Here the label 1, 2 denotes for $(\vec{x}_1, \tau_1), (\vec{x}_2, \tau_2)$, respectively. The hopping strength $t_{\vec{x}_1 \vec{x}_2}$ equals to $-t$ if sites \vec{x}_1, \vec{x}_2 are nearest neighbors and 0 otherwise. One can use the GGW and cGGW equations to solve

the Hubbard model, and the results of such GW method are denoted by GGW and cGGW in the numerical calculation. In the two-dimensional (2D) lattice, we only consider the paramagnetic phase and make the ansatz,

$$\underline{G}(1, 2) = G(1, 2)\underline{\tau}^0, \quad \underline{\Sigma}(1, 2) = \Sigma(1, 2)\underline{\tau}^0, \quad (41)$$

and

$$W^{ab}(1, 2) = W(1, 2)\delta^{ab}, \quad P^{ab}(1, 2) = P(1, 2)\delta^{ab}. \quad (42)$$

One can substitute the paramagnetic ansatz into the GGW equations to obtain the spin-independent Green's function $G(1, 2)$. As for the spin-density vertex $\underline{\Gamma}^a$ (corresponding to the source term $-\int d(1)\phi(1)\sigma^a(1)$) calculation, we make the ansatz $\underline{\Gamma}^a(1, 2, 3) = \Gamma(1, 2, 3)\underline{\tau}^a$ in the cGGW equations, and the spin-spin correlation function can be obtained through such spin-independent vertex $\Gamma(1, 2, 3)$. The details for the calculation in the paramagnetic phase are presented in the Appendix B 3.

B. The Ward-Takahashi identity for the two-dimensional Hubbard model

For the 2D Hubbard lattice system, the WTI related to the $U(1)$ gauge symmetry can be derived as in Sec. II C. The lowest order, i.e., the charge current conservation equation is

$$\begin{aligned} & \frac{\langle \rho(\vec{x}_1, \tau_1) - \rho(\vec{x}_1, \tau_1 - \Delta\tau) \rangle}{\Delta\tau} \\ & - \sum_{\nu} \langle j^{\nu}(x_1, \tau_1) - j^{\nu}(x_1 - e^{\nu}, \tau_1) \rangle \\ & = 0, \end{aligned} \quad (43)$$

where $\nu = x, y$ is the direction of the current. The current operator in the Hubbard system and the density operator corresponding to the discrete time WTI takes the form:

$$\begin{aligned} j^{\nu}(x_1, \tau_1) &= it \sum_{\alpha_1} [\psi_{\alpha_1}^*(x_1, \tau_1) \psi_{\alpha_1}(x_1 + \vec{\tau}_1 e^{\nu}) \\ & - \psi_{\alpha_1}^*(x_1 + \vec{e}^{\nu}, \tau_1) \psi_{\alpha_1}(x_1, \tau_1)], \\ \rho(\vec{x}_1, \tau_1) &= \sum_{\alpha_1} \psi_{\alpha_1}^*(\vec{x}_1, \tau_1) \psi_{\alpha_1}(\vec{x}_1, \tau_1 + \Delta\tau), \end{aligned} \quad (44)$$

and similar to the continuous case, the $U(1)$ WTI at the two-body level is

$$\begin{aligned} & i \sum_{\nu=x,y} [\underline{\Gamma}^{\nu}(1, 2, 3) - \underline{\Gamma}^{\nu}(1, 2, 3 - \vec{e}^{\nu})] \\ & - \frac{\underline{\Gamma}^{\rho}(1, 2, 3) - \underline{\Gamma}^{\rho}(1, 2, 3 - \Delta\tau)}{\Delta\tau} \\ & = \delta(3, 1)\underline{G}^{-1}(3, 2) - \delta(3, 2)\underline{G}^{-1}(1, 3). \end{aligned} \quad (45)$$

One can also prove the cGGW vertex satisfies this equation. The bare vertices in the cGGW equations can be obtained through the current operator kernel $\underline{K}_{j^{\nu}}(1, 2, 3) = it[\delta(1, 2)\delta(3, 1 + \vec{e}^{\nu}) - \delta(1 + e^{\nu}, 2)\delta(1, 3)]\underline{\tau}^0$ and the density operator kernel $\underline{K}_{\rho}(1, 2, 3) = \delta(1, 2)\delta(1 + \delta\tau, 3)\underline{\tau}^0$:

$$\begin{aligned} \underline{\gamma}^{\nu}(1, 2, 3) &= it[\delta(1, 3)\delta(2, 1 + \vec{e}^{\nu}) - \delta(3 + e^{\nu}, 1)\delta(2, 3)]\underline{\tau}^0, \\ \underline{\gamma}^{\rho}(1, 2, 3) &= \delta(2, 1 + \Delta\tau)\delta(1, 3). \end{aligned} \quad (46)$$

Then the cGGW vertex can be solved with Eqs. (12)–(17).

The starting point of the proof is the right-hand side of Eq. (45) and one can rewrite it as Eq. (30). The first term can be rewritten in terms of the bare vertex in the cGGW method:

$$\begin{aligned} & i \sum_{\nu=x,y} [\underline{\gamma}^{\nu}(1, 2, 3) - \underline{\gamma}^{\nu}(1, 2, 3 - \vec{e}^{\nu})] \\ & - \frac{\underline{\gamma}^{\rho}(1, 2, 3) - \underline{\gamma}^{\rho}(1, 2, 3 - \Delta\tau)}{\Delta\tau} \\ & = \delta(3, 1)\underline{T}(3, 2) - \delta(3, 2)\underline{T}(1, 3). \end{aligned} \quad (47)$$

The proof for the MT vertex and AL vertex is the same as the continuous situation, therefore, the cGGW vertex in the Hubbard lattice system preserves the WTI of $U(1)$ symmetry.

In the momentum and frequency space, such a WTI takes the form:

$$\begin{aligned} & i \sum_{\nu} \underline{\Gamma}^{\nu}(p, q)[1 - e^{iq^{\nu}}] + \frac{e^{-i\pi 2m_q/M} - 1}{\Delta\tau} \underline{\Gamma}^{\rho}(p, q) \\ & = \underline{G}^{-1}(p) - \underline{G}^{-1}(p + q). \end{aligned} \quad (48)$$

Here Γ^{ν}, Γ^0 are the current vertex and the charge vertex. The fermionic momentum and Matsubara frequency are denoted by $p = ((p_x, p_y), \omega_p = (2m_p + 1)\pi T)$, and the bosonic momentum and Matsubara frequency are denoted by $q = ((q_x, q_y), \omega_q = 2m_q\pi T)$. The equation above establishes a relation between the vertex $\underline{\Gamma}^{\nu}, \underline{\Gamma}^{\rho}$ and the Green's function, and represents the charge current conservation law at the two-body level in the Hubbard model.

IV. cGGW NUMERICAL RESULTS FOR THE TWO-DIMENSIONAL HUBBARD MODEL

A. Numerical verification of preserving the WTI and FDT

We numerically verify our approach preserves the FDT and WTI on the 16×16 half-filled lattice with $U = 2$ for different temperatures.

The FDT relates the response function to the correlation function. We focus on the static antiferromagnetic spin susceptibility and the spin-spin correlation function χ_{sp} at momentum $\vec{Q} = (\pi, \pi)$ in the Hubbard model, which satisfy the equality as required by the FDT [20],

$$\left. \frac{\partial m}{\partial h} \right|_{h=0} = \chi_{sp}(\vec{Q}, i\omega_n = 0), \quad (49)$$

where h is the staggered field, m is the staggered magnetization, and $\chi_{sp}(p)$ is the spin-spin correlation. We directly calculate the static antiferromagnetic susceptibility ($\partial m/\partial h$) by adding a staggered field h in the GGW equations, and compared it with the spin-spin correlation function χ_{sp} obtained from different methods. It is found that only the cGGW method preserves the FDT at all temperature ranges, as shown in Fig. 2(a). However, the RPA and BSE methods lead to a violation of the FDT, and the BSE is even more destructive to the FDT.

We measure the deviation of the WTI by

$$D(p, q) = \left\| \frac{\text{Tr}[LHS(p, q) - RHS(p, q)]}{\text{Tr}[LHS(p, q)]} \right\|, \quad (50)$$

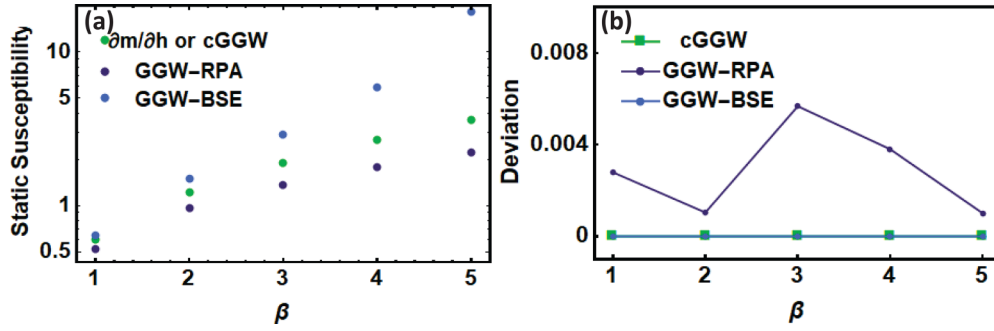


FIG. 2. (a) The comparison of the static antiferromagnetic spin susceptibility obtained by $\frac{\partial m}{\partial h}|_{h=0}$, cGGW, GGW-RPA, and GGW-BSE. Only the cGGW respects the FDT. (b) shows the deviation $D(p, q)$ of the WTI with momentum $\vec{p} = (\pi/2, \pi/2)$, $\vec{q} = (\pi, \pi)$ and frequencies $m_p = 1, m_q = 2$ obtained by cGGW, GGW-RPA, and GGW-BSE. The deviation for cGGW and GGW-BSE are 0, while GGW-RPA are not.

where (*LHS*) and (*RHS*) are the left- and the right-hand sides in Eq. (48), and the results are shown in Fig. 2(b). The deviations $D(p, q)$ calculated by the cGGW and BSE approaches are negligible, which means preserving the WTI as expected. Meanwhile, the GGW-RPA violates the WTI significantly, indicating a rather poor description of conservation laws.

B. Antiferromagnetic susceptibility compared with other methods

To demonstrate the effectiveness of the method, we compare the antiferromagnetic susceptibility from the cGGW method with that obtained from the DQMC method [26–28], which is numerically exact and often serves as a benchmark for approximate methods. As a prototypical example, here we set a typical value of $U = 2$ for the static results, so as to compare with previous studies of the 2D Hubbard model using multiple methods [29].

We consider the case at half-filling and away from half-filling for different interacting strengths ($U = 2$ and 4) in Fig. 3. For the weak-coupling $U = 2$, all the approaches in the Fig. 3 can obtain good imaginary time antiferromagnetic susceptibility results compared to the DQMC benchmark, and the cGGW exhibits more precise results than the GH-RPA and the GGW-RPA. For the immediate coupling $U = 4$ at half-filling, all these approaches cannot obtain precise enough susceptibilities, while the cGGW presents a significant improvement over the GGW-RPA. For the coupling $U = 4$ at filling $n = 0.918$, only the cGGW exhibits a highly precise agreement in comparison to the benchmark. However, the GH-RPA results diverge for $U = 4$ at both fillings, i.e., the GH-RPA predicts an incorrect broken phase. It should be noted that, the analytic continuation to real time is extremely sensitive to some features of the imaginary time susceptibility, such as the slope of the $\chi_{sp}(\tau)$ in the $\tau \rightarrow 0$ limit $\chi'_{sp}(\tau \rightarrow 0)$ and the $\chi_{sp}(\tau = \frac{\beta}{2})$. For the deviation of $\chi'_{sp}(\tau \rightarrow 0)$ from DQMC, the cGGW results remain near 4% for all these parameters, while the GGW-RPA results show near 9% for $U = 2$ and near 30% for $U = 4$, the GH-RPA show near 7% for $U = 2$ and diverge for $U = 4$. As for the deviation of $\chi_{sp}(\tau = \frac{\beta}{2})$ from DQMC, the cGGW results remain below 6% in Figs. 3(a), 3(b), and 3(d) and show 36% in Fig. 3(c), while the GGW-RPA results present above 35% for $U = 2$ and above 55% for $U = 4$, the GH-RPA show above 11% for $U = 2$ and diverge for $U = 4$.

The corresponding data is shown in Appendix B 4. Thus, for the covariant spin fluctuation calculation, the GGW approximation is better than the generalized Hartree approximation, especially for the immediate or the stronger coupling. And for the GGW approximation, the covariant approach can improve the accuracy of the susceptibilities significantly compared to the RPA formula.

To calculate the static antiferromagnetic susceptibility for infinite lattice, we use the finite-size scaling to approach the thermodynamic limit and choose samples with lattice sizes from $L = 32$ to $L = 128$. We take time slices M of 8 values from 512 to 2048, extrapolating to infinite M results. Figure 4 shows $\chi_{sp}(\vec{Q}, i\omega_n = 0)$ for various methods as a function of the inverse temperatures on a logarithmic scale. The cGGW curve (green line) displays a quantitative agreement with the numerically exact DQMC method (red line) until $\beta \approx 8$. Since the thermodynamic transition manifests itself as a divergence of the susceptibility at the corresponding wave vector, our cGGW results also indicate an antiferromagnetic transition at ($\beta \approx 13.1$). Figure 4(a) demonstrates that the cGGW and GH-RPA present similar results, and are much better than the GGW-RPA. Figure 4(b) shows the cGGW result is comparable with the DMFT or cellular DMFT (CDMFT) methods which, however, usually require expensive computational costs. By contrast, the computational complexity of the cGGW susceptibility at a specific momentum is $\mathcal{O}(L^d M \log(LM))$, with d the lattice dimension. For a typical parameter set in the discussion (lattice size 16×16 , time slices $M = 1024$), the numerical cost of calculation for spin fluctuation for a single momentum and frequency is only 3.11 seconds on a 4-core CPU(1.8GHz), indicating a computationally efficient method.

It should be noted that the generalized Hartree-RPA calculation, preserving both the WTI and the FDT, can obtain accurate susceptibility results for the small U case. However, the GH-RPA for the larger U sometimes leads to failure at a qualitative level, which can be overcome by a higher-order approximation, such as cGGW.

V. CONCLUSION

We presented the formalism of the functional derivative scheme based on the GGW method for a general action, and theoretically proved that this scheme preserves the WTI. We

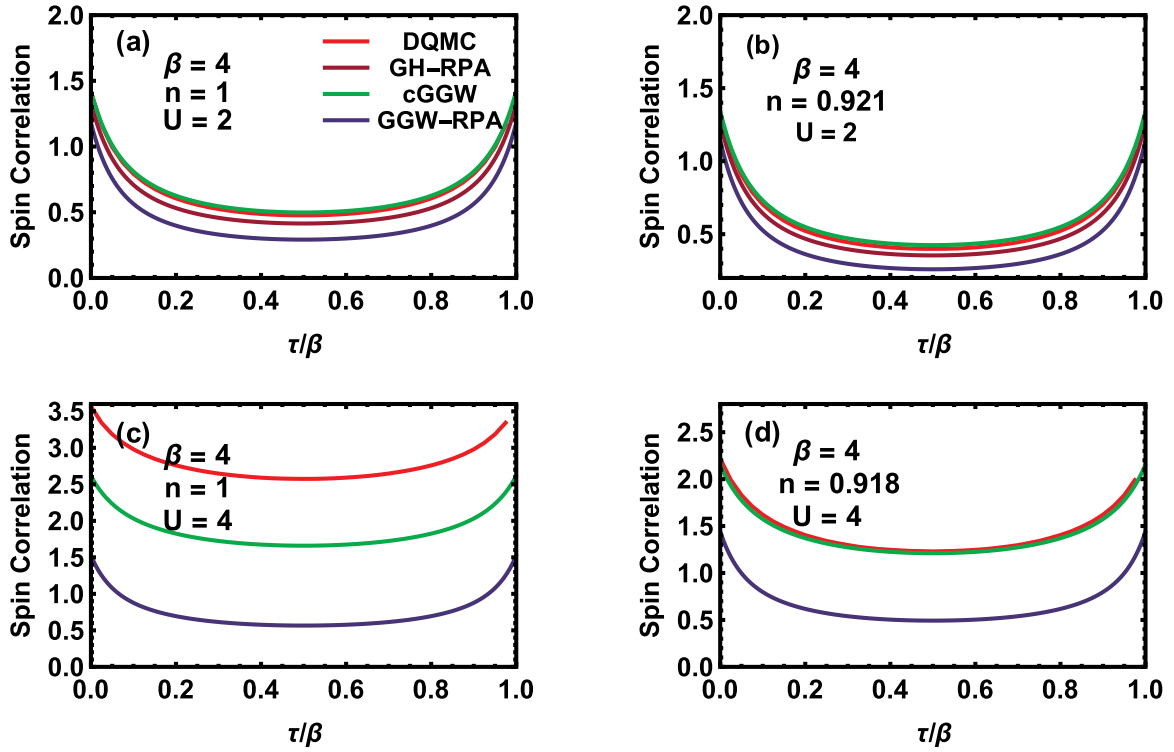


FIG. 3. Antiferromagnetic spin susceptibility $\chi_{sp}(\vec{k} = \vec{Q}, \tau)$ as a function of imaginary time for DQMC, cGGW, GH-RPA, traditional GW-RPA and GGW-RPA at $\beta = 4$ for different parameters: (a) $U = 2, n = 1$, (b) $U = 2, n = 0.921$, (c) $U = 4, n = 1$, (d) $U = 4, n = 0.918$. The error of DQMC is 10^{-3} , other methods are all calculated through the discrete time algorithm with $L = 16$ and $M = 1024$ (almost M reaches to infinite limit). In (c) and (d), the GH-RPA results diverge, so the corresponding curves are not shown.

numerically verified that this scheme satisfies both the WTI and the FDT in the 2D Hubbard model. At the same time, we calculated the deviations of the commonly used RPA and BSE from the WTI and FDT. We found that RPA has an obvious deviations from both two equalities, and BSE satisfies WTI but violates the FDT.

We numerically calculated the antiferromagnetic spin-spin correlation function at the Matsubara time axis within GGW-RPA, GH-RPA, and the cGGW methods, and compared them with the numerically exact results obtained by the DQMC simulations. The GH-RPA also yields a pretty good result in the weak-coupling cases, and cGGW only makes a slight improvement. Both in the weak and intermediate coupling cases,

the results show that the cGGW method makes a significant improvement over the GGW-RPA method. We also calculated the antiferromagnetic spin susceptibility at half-filling and weak coupling for different temperatures, and compared the result with those obtained by DQMC, DMFT, and CDMFT approaches. The results show that the cGGW method can compete with the DMFT calculation within the range of parameters considered.

Due to the acceptable computational cost and numerical quality, the cGGW method is expected to be applied in realistic material computation in the future for the calculations of the various susceptibilities, especially the transport properties of the correlated systems with spin-dependent interaction.

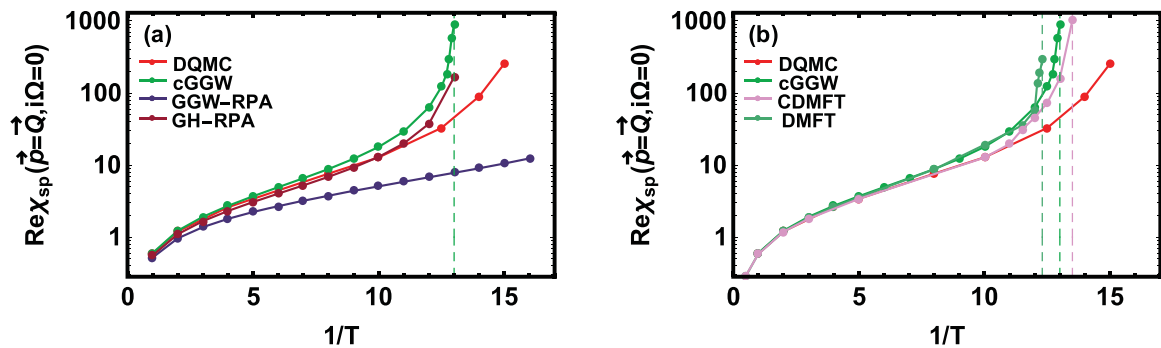


FIG. 4. Antiferromagnetic static susceptibility $\chi_{sp}(\vec{k} = \vec{Q}, i\omega_n = 0)$ as a function of (inverse) temperature on a logarithmic scale at $U = 2$ and $n = 1$ in the thermodynamic limit for various methods: (a) cGGW, DQMC, GGW-RPA, GH-RPA; (b) cGGW, DQMC, DMFT, CDMFT. Data of DQMC, DMFT, CDMFT ($N_c = 8 \times 8$) is taken from Ref. [29].

ACKNOWLEDGMENTS

This work is supported by the National Natural Science Foundation of China (Grant No. 12174006) and High-performance Computing Platform of Peking University. H.H. acknowledges the support of the National Key R&D Program

of China (No. 2021YFA1401600), the National Natural Science Foundation of China (Grant No. 12074006), and the start-up fund from Peking University. The authors are very grateful to B. Rosenstein, T. Ma, H. Jiang, X. Ren, and Z. Fan for valuable discussions and help in numerical computations.

APPENDIX A: WARD-TAKAHASHI IDENTITY

1. Derivation of Ward-Takahashi identity

The invariance of the functional integral measure $D[\psi^*, \psi]$ under the infinitesimal gauge transformation of the complex field yields an equality

$$\delta \int D[\psi^*, \psi] \mathcal{F}[\psi^*, \psi] e^{-S[\psi^*, \psi]} = 0, \quad (\text{A1})$$

with \mathcal{F} an arbitrary functional, which is identical to

$$\sum_{\alpha_1} \int D[\psi^*, \psi] \left[\delta \psi_{\alpha_1}^*(1) \frac{\delta}{\delta \psi_{\alpha_1}^*(1)} + \delta \psi_{\alpha_1}(1) \frac{\delta}{\delta \psi_{\alpha_1}(1)} \right] \mathcal{F}[\psi^*, \psi] e^{-S} = 0. \quad (\text{A2})$$

Consider the infinitesimal $U(1)$ transformation,

$$\psi_{\alpha_1}^*(1) \rightarrow \psi_{\alpha_1}^*(1) e^{i\delta\theta}, \quad \psi_{\alpha_1}(1) \rightarrow \psi_{\alpha_1}(1) e^{-i\delta\theta}, \quad (\text{A3})$$

where $\delta\theta$ is the infinitesimal phase, one can obtain

$$\sum_{\alpha_1} \int D[\psi^*, \psi] \left[\psi_{\alpha_1}^*(1) \frac{\delta}{\delta \psi_{\alpha_1}^*(1)} - \psi_{\alpha_1}(1) \frac{\delta}{\delta \psi_{\alpha_1}(1)} \right] \mathcal{F}[\psi^*, \psi] e^{-S} = 0. \quad (\text{A4})$$

Letting $\mathcal{F} = 1$ in Eq. (A4) yields the WTI for the one-body Green's function:

$$\int d(2) \text{Tr}[\underline{T}(1, 2) \underline{G}(2, 1)] = \int d(2) \text{Tr}[\underline{T}(2, 1) \underline{G}(1, 2)]. \quad (\text{A5})$$

Letting $\mathcal{F} = \psi_{\alpha_3}^*(3) \psi_{\alpha_2}(2)$ yields the WTI for the two-body Green's function:

$$\begin{aligned} & \sum_{\alpha_1 \beta_4} \int d(4) T_{\alpha_1 \beta_4}(1, 4) \langle \psi_{\alpha_3}^*(3) \psi_{\alpha_2}(2) \psi_{\alpha_1}^*(1) \psi_{\beta_4}(4) \rangle - \sum_{\alpha_1 \beta_4} \int d(4) T_{\beta_4 \alpha_1}(4, 1) \langle \psi_{\alpha_3}^*(3) \psi_{\alpha_2}(2) \psi_{\beta_4}^*(4) \psi_{\alpha_1}(1) \rangle \\ & = - \sum_{\alpha_1} (\delta(1, 3) \delta_{\alpha_1 \alpha_3} - \delta(1, 2) \delta_{\alpha_1 \alpha_2}) G_{\alpha_2 \alpha_3}(2, 3). \end{aligned} \quad (\text{A6})$$

For the continuous system with T -term Eq. (20), the equations above can be rewritten as Eqs. (21) an (24).

2. Preserving of the Ward-Takahashi identity within cGGW

In the main text, we find the first term and the third term in the right-hand side of Eq. (34) equals to $\Gamma_1^{\text{WTI}}(1, 2, 3)$, $\Gamma_2^{\text{WTI}}(1, 2, 3)$. Now we prove other terms in the right hand of side in Eq. (34) equal to 0.

We can define

$$\Gamma_3^{\text{WTI}} \equiv \delta(1, 2) \sum_{cd} \int d(456) \underline{\tau}^c V^{cd}(1, 4) \text{Tr}[\underline{\tau}^d \underline{G}(1, 5)] \left[\sum_{\nu_3} \partial_{\nu_3} \Gamma^{\nu_3}(5, 6, 3) - \partial_{\tau_3} \Gamma^\rho(5, 6, 3) \right] \underline{G}(6, 2). \quad (\text{A7})$$

Substituting the WTI (25) in to Eq. (A7), one can obtain

$$\delta(1, 2) \sum_{cd} \int d(456) \underline{\tau}^c V^{cd}(1, 4) \text{Tr}[\underline{\tau}^d \underline{G}(1, 5)] (\delta(3, 5) \underline{G}^{-1}(3, 6) - \delta(3, 6) \underline{G}^{-1}(5, 3)) \underline{G}(6, 2) = 0, \quad (\text{A8})$$

and we define

$$\Gamma_4^{\text{WTI}} \equiv - \sum_{cdef} \int d(567) \underline{\tau}^c \underline{G}(1, 2) \underline{\tau}^d W^{de}(1, 4) \Omega W^{fc}(5, 2), \quad (\text{A9})$$

where

$$\begin{aligned} \Omega \equiv & \int d(567) \text{Tr}[\underline{\tau}^e \underline{G}(4, 6) \left[\sum_{\nu_3} \partial_{\nu_3} \underline{\Gamma}^{\nu_3}(6, 7, 3) - \partial_{\tau_3} \underline{\Gamma}^\rho(6, 7, 3) \right] \underline{G}(7, 5) \underline{\tau}^f \underline{G}(5, 4) \\ & + \underline{\tau}^e \underline{G}(4, 5) \underline{\tau}^f \underline{G}(5, 6) \left[\sum_{\nu_3} \partial_{\nu_3} \underline{\Gamma}^{\nu_3}(6, 7, 3) - \partial_{\tau_3} \underline{\Gamma}^\rho(6, 7, 3) \right] \underline{G}(7, 4)]. \end{aligned} \quad (\text{A10})$$

Substituting the WTI (25) in to Eq. (A10), one can obtain

$$\begin{aligned} & \int d(567) \text{Tr}[\underline{\tau}^e \underline{G}(4, 6) [-\delta(3, 6) \underline{G}^{-1}(3, 7) + \delta(3, 7) \underline{G}^{-1}(6, 3)] \underline{G}(7, 5) \underline{\tau}^f \underline{G}(5, 4) \\ & + \underline{\tau}^e \underline{G}(4, 5) \underline{\tau}^f \underline{G}(5, 6) [-\delta(3, 6) \underline{G}^{-1}(3, 7) + \delta(3, 7) \underline{G}^{-1}(6, 3)] \underline{G}(7, 4)] = 0. \end{aligned} \quad (\text{A11})$$

So, for the GGW Green's function, the WTI (25) is identical to

$$\sum_{\nu_3} \partial_{\nu_3} \underline{\Gamma}^{\nu_3}(1, 2, 3) - \partial_{\tau_3} \underline{\Gamma}^0(1, 2, 3) = \Gamma_1^{WTI} + \Gamma_2^{WTI} + \Gamma_3^{WTI} + \Gamma_4^{WTI}, \quad (\text{A12})$$

and one can notice the cGGW vertex and BSE vertex satisfy the WTI automatically.

APPENDIX B: IMPLEMENTATION IN THE TWO-DIMENSIONAL HUBBARD MODEL

1. Fourier transformation for a translational invariant lattice

For a lattice with the translation symmetries, we use the discrete Fourier transformation to simplify our equations. The Fermionic array X_F takes the form

$$X_F(1, 2) = \frac{1}{\mathcal{N}} \sum_k X_F(k) \mathcal{E}_F(k, 1-2), \quad (\text{B1})$$

and the Bosonic array X_B takes the form

$$X_B(1, 2) = \frac{1}{\mathcal{N}} \sum_k X_B(k) \mathcal{E}_B(k, 1-2). \quad (\text{B2})$$

Here the transformation kernels \mathcal{E}_F and \mathcal{E}_B are defined as

$$\mathcal{E}_F(k, 1-2) \equiv e^{i\vec{k} \cdot (\vec{x}_1 - \vec{x}_2)} e^{-i \frac{2m_k+1}{M} (l_1 - l_2)}, \quad (\text{B3})$$

$$\mathcal{E}_B(k, 1-2) \equiv e^{i\vec{k} \cdot (\vec{x}_1 - \vec{x}_2)} e^{-i \frac{2m_k}{M} (l_1 - l_2)}, \quad (\text{B4})$$

respectively. Here $\mathcal{N} = \beta L^2$, $k = (\vec{k}, m_k)$ and m_k takes the integer value from 0 to $M-1$. Note that the transformation of the T term is

$$\underline{T}(k) = \left[-\frac{1}{\Delta\tau} (e^{-i\pi(2m_k+1)/M} - 1) - \varepsilon(\vec{k}) + \mu \right] \underline{\tau}^0, \quad (\text{B5})$$

with $\varepsilon(\vec{k})$ the noninteracting dispersion. For the two-dimensional Hubbard model, $\varepsilon(\vec{k}) = -2t(\cos k_x + \cos k_y)$ with t the nearest-neighbor hopping strength.

2. GGW and covariant GGW equations in Fourier space

Note that the one-body Green's function \underline{G} and the self-energy $\underline{\Sigma}$ are Fermionic arrays, and the dynamical potential W^{ab} and the polarization P^{ab} are Bosonic arrays. It is easy to

derive the GGW equations in Fourier space

$$\underline{G}^{-1}(k) = \underline{T}^{-1}(k) - \underline{\Sigma}_H(k) - \underline{\Sigma}(k),$$

$$\underline{\Sigma}(k) = -\frac{1}{\mathcal{N}} \sum_{q, ab} \underline{\tau}^a \underline{G}(k+q) \underline{\tau}^b W^{ba}(q),$$

$$(W^{-1})^{ab}(q) = (V^{-1})^{ab}(q) - P^{ab}(q),$$

$$P^{ab}(q) = \frac{1}{\mathcal{N}} \sum_k \text{Tr}[\underline{\tau}^a \underline{G}(q+k) \underline{\tau}^b \underline{G}(q)]. \quad (\text{B6})$$

To derive the covariant GGW equations in Fourier space, we first make ansatz for the vertex function

$$\underline{\Gamma}(1, 2, 3) = \frac{1}{\mathcal{N}^2} \sum_{p, q} \underline{\Gamma}(p, q) \mathcal{E}_F(k, 1-2) \mathcal{E}_B(q, 1-3). \quad (\text{B7})$$

Then one obtains

$$\begin{aligned} \underline{\Gamma}(p, q) = & \underline{\gamma}(p, q) + \underline{\Gamma}_H(p, q) + \underline{\Gamma}_{MT}(p, q) \\ & + \underline{\Gamma}_{AL1}(p, q) + \underline{\Gamma}_{AL2}(p, q). \end{aligned} \quad (\text{B8})$$

The bare vertex is

$$\underline{\gamma}(p, q) = \underline{K}(-p-q, p). \quad (\text{B9})$$

The bubble vertex is

$$\underline{\Gamma}_H(p, q) = \frac{1}{\mathcal{N}} \sum_{cd} \sum_k \underline{\tau}^c V^{cd}(q) \text{Tr}[\underline{\tau}^d \underline{G}(k+q) \underline{\Gamma}(k, q) \underline{G}(k)]. \quad (\text{B10})$$

The MT vertex is

$$\begin{aligned} \underline{\Gamma}_{MT}(p, q) = & -\frac{1}{\mathcal{N}} \sum_{cd} \sum_k \underline{\tau}^c \underline{G}(p+k+q) \\ & \times \underline{\Gamma}(p+k, q) \underline{G}(p+k) \underline{\tau}^d W^{dc}(k). \end{aligned} \quad (\text{B11})$$

The two AL vertices are

$$\begin{aligned} \Gamma_{\text{AL1}}(k, q) = & -\frac{1}{\mathcal{N}^2} \sum_{cdef} \sum_{kk'} \underline{\tau}^c \underline{G}(p+q+k) \\ & \times \underline{\tau}^d W^{de}(k+q) W^{fc}(k) \\ & \times \text{Tr}[\underline{\tau}^e \underline{G}(k+k'+q) \underline{\Gamma}(k+k', q)] \\ & \times \underline{G}(k+k') \underline{\tau}^f \underline{G}(k'), \end{aligned} \quad (\text{B12})$$

$$\begin{aligned} \Gamma_{\text{AL2}}(k, q) = & -\frac{1}{\mathcal{N}^2} \sum_{cdef} \sum_{kk'} \underline{\tau}^c \underline{G}(p+q+k) \\ & \times \underline{\tau}^d W^{de}(k+q) W^{fc}(k) \\ & \times \text{Tr}[\underline{\tau}^e \underline{G}(k+q+k') \underline{\tau}^f \underline{G}(k'+q)] \\ & \times \underline{\Gamma}(k', q) \underline{G}(k'). \end{aligned} \quad (\text{B13})$$

The diagrammatics for these vertices are presented in Fig. 1. Note that in the RPA, the vertex is given by

$$\begin{aligned} \underline{\Gamma}_{\text{RPA}}(p, q) = & \underline{\gamma}(p, q) + \frac{1}{\mathcal{N}} \sum_{cd} \sum_k \underline{\tau}^c V^{cd}(q) \\ & \times \text{Tr}[\underline{\tau}^d \underline{G}(k+q) \underline{\Gamma}_{\text{RPA}}(k, q) \underline{G}(k)]. \end{aligned} \quad (\text{B14})$$

The RPA formula is usually used to calculate the density-density or spin-spin correlation functions. In the Bethe-Salpeter equation approach, the MT vertex is taken into account, but the AL vertices are neglected.

3. GGW and covariant GGW equations for the 2D Hubbard model

For the 2D Hubbard model, $\underline{T}(k)$ takes the form $T(k)\underline{\tau}^0$ and $V^{ab}(k)$ takes the form $I^s \delta^{ab}$ with a, b taking values of x, y, z . To find the paramagnetic solutions, we can make the ansatz

$$\underline{G}(k) = G(k)\underline{\tau}^0, \quad \underline{\Sigma}(k) = \Sigma(k)\underline{\tau}^0, \quad (\text{B15})$$

and

$$W^{ab}(k) = W(k)\delta^{ab}, \quad P^{ab}(k) = P(k)\delta^{ab}. \quad (\text{B16})$$

The GGW equation is then simplified as

$$\begin{aligned} G^{-1}(k) = & T(k) - \Sigma(k), \quad \Sigma(k) = -\frac{3}{\mathcal{N}} \sum_q G(k+q)W(q), \\ W^{-1}(q) = & 1/I^s - P(q), \quad P(q) = \frac{2}{\mathcal{N}} \sum_k G(p+k)G(p). \end{aligned} \quad (\text{B17})$$

The simplification of the covariant GGW equations related to the species of correlation functions. We take the spin-spin correlation function as an example here. The spin-spin correlation function $\chi_s^{ab}(p)$ relates to the vertex function through

$$\chi_s^{ab}(p) = -\sum_q \text{Tr}[\underline{G}(p+q) \underline{\Gamma}^a(q, p) \underline{G}(q) \tau^b]. \quad (\text{B18})$$

Here $\underline{\Gamma}^a$ refers to the vertex function corresponding to the spin operator σ^a . By the ansatz $\underline{\Gamma}^a(q, p) = \underline{\tau}^a \Gamma(q, p)$, the spin-spin correlation function $\chi_s^{ab}(p) = -2\delta^{ab} \sum_q G(p+$

TABLE I. The deviation of $\chi(\tau = 0)$ from D QMC.

Parameters	cGGW	GGW-RPA	GH-RPA
$U=2, n=1$	0.00026	0.172	0.0661
$U=2, n=0.921$	0.00792	0.145	0.0522
$U=4, n=1$	0.270	0.576	diverge
$U=4, n=0.918$	0.0321	0.355	diverge

$q)\Gamma(p, q)G(q)$, and the equation for the vertex function is simplified as

$$\begin{aligned} \Gamma(p, q) = & \gamma(p, q) + \Gamma_{\text{H}}(p, q) + \Gamma_{\text{MT}}(p, q) \\ & + \Gamma_{\text{AL1}}(p, q) + \Gamma_{\text{AL2}}(p, q), \end{aligned} \quad (\text{B19})$$

with the bare vertex $\gamma(p, q) = 1$, the ‘‘bubble’’ vertex

$$\Gamma_{\text{H}}(p, q) = \frac{2I^s}{\mathcal{N}} \sum_k G(k+q)\Gamma(k, q)G(k), \quad (\text{B20})$$

the MT vertex

$$\begin{aligned} \Gamma_{\text{MT}}(p, q) = & -\frac{1}{\mathcal{N}} \sum_k G(p+k+q)\Gamma(p+k, q)G(p+k)W(k), \end{aligned} \quad (\text{B21})$$

and two AL vertices

$$\begin{aligned} \Gamma_{\text{AL1}}(p, q) = & \frac{2}{\mathcal{N}^2} \sum_{kk'} G(p+q+k)W(k+q)G(k+k'+q) \\ & \times \Gamma(k+k', q)G(k+k')G(k')W(k), \quad (\text{B22}) \\ \Gamma_{\text{AL2}}(p, q) = & -\frac{2}{\mathcal{N}^2} \sum_{kk'} G(p+q+k)W(k+q) \\ & \times G(k+k'+q)G(k'+q)\Gamma(k', q)G(k')W(k). \end{aligned} \quad (\text{B23})$$

As for the density case, the density-density correlation function relates the vertex through

$$\chi_\rho(p) = \sum_q \text{Tr}[\underline{G}(p+q) \underline{\Gamma}^\rho(q, p) \underline{G}(q) \tau^0], \quad (\text{B24})$$

$\underline{\Gamma}^\rho$ here refers to the charge vertex. With the ansatz $\underline{\Gamma}^\rho = \underline{\tau}^0 \Gamma^\rho$, the density-density can be evaluate through $\chi_\rho(p) = 2 \sum_q G(p+q)\Gamma^\rho(q, p)G(q)$. The equation for the vertex is simplified as

$$\begin{aligned} \Gamma^\rho(p, q) = & \gamma^\rho(p, q) + \Gamma_{\text{H}}^\rho(p, q) + \Gamma_{\text{MT}}^\rho(p, q) \\ & + \Gamma_{\text{AL1}}^\rho(p, q) + \Gamma_{\text{AL2}}^\rho(p, q), \end{aligned} \quad (\text{B25})$$

with the bare vertex $\gamma^\rho(p, q) = 1$, the ‘‘bubble’’ vertex $\Gamma_{\text{H}}^\rho(p, q) = 0$, and the MT vertex

$$\begin{aligned} \Gamma_{\text{MT}}^\rho(p, q) = & -\frac{3}{\mathcal{N}} \sum_k G(p+k+q)\Gamma^\rho(p+k, q)G(p+k)W(k), \end{aligned} \quad (\text{B26})$$

TABLE II. The deviation of $\chi'(\tau = 0)$ from DQMC.

Parameters	cGGW	GGW-RPA	GH-RPA
$U=2, n=1$	0.035	0.095	0.070
$U=2, n=0.921$	0.038	0.097	0.073
$U=4, n=1$	0.049	0.322	diverge
$U=4, n=0.918$	0.033	0.298	diverge

and two AL vertices

$$\Gamma_{\text{AL1}}^\rho(p, q) = -\frac{6}{\mathcal{N}^2} \sum_{kk'} G(p+q+k)W(k+q)G(k+k'+q) \\ \times \Gamma^\rho(k+k', q)G(k+k')G(k')W(k), \quad (\text{B27})$$

$$\Gamma_{\text{AL2}}^\rho(p, q) = -\frac{6}{\mathcal{N}^2} \sum_{kk'} G(p+q+k)W(k+q) \\ \times G(k+k'+q)G(k'+q)\Gamma^\rho(k', q)G(k')W(k). \quad (\text{B28})$$

As for the current case, the current-current correlation function relates the vertex through

$$\chi_{jj}^{vv'}(p) = it \sum_q \text{Tr}[\underline{G}(p+q)\underline{\Gamma}^{v'}(q, p)\underline{G}(q)\tau^0] \\ \times (e^{-iq^{v'}} - e^{iq^{v'} + ip^{v'}}). \quad (\text{B29})$$

$\underline{\Gamma}^v$ refers to the current vertex along the lattice vector \bar{e}^v . With the ansatz $\underline{\Gamma}^v = \underline{\tau}^0 \Gamma^v$, the current-current can be evaluate through $\chi_{jj}^{vv'}(p) = 2it \sum_q G(p+q)\Gamma^{v'}(q, p)G(q)(e^{-iq^{v'}} - e^{iq^{v'} + ip^{v'}})$. The cGGW vertex is simplified as

$$\Gamma^v(p, q) = \gamma^v(p, q) + \Gamma_{\text{H}}^v(p, q) + \Gamma_{\text{MT}}^v(p, q) \\ + \Gamma_{\text{AL1}}^v(p, q) + \Gamma_{\text{AL2}}^v(p, q), \quad (\text{B30})$$

with the bare vertex $\gamma^v(p, q) = it[e^{-i(p_1^v + p_2^v)} - e^{ip_1^v}]$, the ‘‘bubble’’ vertex $\Gamma_{\text{H}}^v(p, q) = 0$, and the MT vertex

$$\Gamma_{\text{MT}}^v(p, q) \\ = -\frac{3}{\mathcal{N}} \sum_k G(p+k+q)\Gamma^v(p+k, q)G(p+k)W(k), \quad (\text{B31})$$

and two AL vertices

$$\Gamma_{\text{AL1}}^v(p, q) = -\frac{6}{\mathcal{N}^2} \sum_{kk'} G(p+q+k) \\ \times W(k+q)G(k+k'+q) \\ \times \Gamma^v(k+k', q)G(k+k')G(k')W(k), \quad (\text{B32})$$

TABLE III. The deviation of $\chi(\tau = \beta/2)$ from DQMC.

Parameters	cGGW	GGW-RPA	GH-RPA
$U=2, n=1$	0.0463	0.388	0.130
$U=2, n=0.921$	0.0643	0.350	0.112
$U=4, n=1$	0.355	0.780	diverge
$U=4, n=0.918$	0.0154	0.599	diverge

TABLE IV. DQMC data (Errors are around 10^{-3}).

Parameters	$\chi(\tau = 0)$	$\chi'(\tau = 0)$	$\chi(\tau = \beta/2)$
$U=2, n=1$	1.41	2.87	0.476
$U=2, n=0.921$	1.32	2.86	0.399
$U=4, n=1$	3.57	2.54	2.57
$U=4, n=0.918$	2.22	2.58	1.23

$$\Gamma_{\text{AL2}}^v(p, q) = -\frac{6}{\mathcal{N}^2} \sum_{kk'} G(p+q+k)W(k+q)G(k+k'+q) \\ \times G(k'+q)\Gamma^v(k', q)G(k')W(k). \quad (\text{B33})$$

Note that the calculation can be fasten by discrete Fourier transformation algorithm, and as a result, the computational complexity of the cGGW susceptibility at a specific momentum is $\mathcal{O}(L^d M \log(LM))$, with d the lattice dimension.

4. Details of the imaginary time spin correlation functions

In the description of Fig. 3, we state the slope of the $\chi_{sp}(\tau)$ in the $\tau \rightarrow 0$ limit $\chi'_{sp}(\tau \rightarrow 0)$ and the $\chi_{sp}(\tau = \frac{\beta}{2})$ are important to the analytic continuation. Here we present the corresponding data in Tables I, II, III, and IV.

APPENDIX C: TRADITIONAL GW

1. The GW and covariant GW equations

For the Hamiltonian Eq. (35), one can derive the traditional GW equations from the lowest order of the Hedin's equations, where the Hartree self-energy, self-energy and the effective potential take the form:

$$\Sigma_H^{GW}(\bar{1}, \bar{2}) = -\delta(\bar{1}, \bar{2}) \int d\bar{3} V(\bar{1}, \bar{3})G(\bar{3}, \bar{3}), \quad (\text{C1})$$

$$\Sigma^{GW}(\bar{1}, \bar{2}) = -G(\bar{1}, \bar{2})W(\bar{2}, \bar{1}), \quad (\text{C2})$$

$$W^{-1}(\bar{1}, \bar{2}) = V^{-1}(\bar{1}, \bar{2}) - G(\bar{1}, \bar{2})G(\bar{2}, \bar{1}), \quad (\text{C3})$$

where $\bar{1} = (\sigma_1, 1) = (\sigma_1, \bar{x}_1, \tau_1)$ and $V(\bar{1}, \bar{2}) = U\delta(1, 2)\delta_{\sigma_1, -\sigma_2}$. The covariant and RPA correlation functions can be derived with the same procedure in the Sec. II B.

$$\Gamma_H(\bar{1}, \bar{2}, 3) \\ = \delta(\bar{1}, \bar{2}) \int d(\bar{4}\bar{5}\bar{6})V(\bar{1}, \bar{4})G(\bar{4}, \bar{5})\Gamma(\bar{5}, \bar{6}, 3)G(\bar{6}, \bar{4}), \quad (\text{C4})$$

$$\Gamma_{\text{MT}}(\bar{1}, \bar{2}, 3) = -\int d(\bar{4}\bar{5})G(\bar{1}, \bar{4})\Gamma(\bar{4}, \bar{5}, 3)G(\bar{5}, \bar{2})W(\bar{2}, \bar{1}), \quad (\text{C5})$$

$$\Gamma_{\text{AL1}}(\bar{1}, \bar{2}, 3) = -\int d(\bar{4}\bar{5}\bar{6}\bar{7})G(\bar{1}, \bar{2})W(\bar{1}, \bar{4})G(\bar{4}, \bar{6})\Gamma \\ \times (\bar{6}, \bar{7}, 3)G(\bar{7}, \bar{5})G(\bar{5}, \bar{4})W(\bar{5}, \bar{2}), \quad (\text{C6})$$

$$\Gamma_{\text{AL2}}(\bar{1}, \bar{2}, 3) = -\int d(\bar{4}\bar{5}\bar{6}\bar{7})G(\bar{1}, \bar{2})W(\bar{1}, \bar{4})G(\bar{4}, \bar{5})G(\bar{5}, \bar{6}) \\ \times \Gamma(\bar{6}, \bar{7}, 3)G(\bar{7}, \bar{4})W(\bar{5}, \bar{2}). \quad (\text{C7})$$

The response function can be obtained from such self-consistent vertex through Eq. (18).

2. Numerical results

There is the SU(2) gauge symmetry in the Hubbard model, and accordingly, the spin-spin correlation functions in the different directions need to be equal in the para-phase. We compare the static antiferromagnetic susceptibility $\chi_{sp}^{xx}(\vec{Q}, i\omega_n = 0)$, $\chi_{sp}^{yy}(\vec{Q}, i\omega_n = 0)$, $\chi_{sp}^{zz}(\vec{Q}, i\omega_n = 0)$ in Fig. 5 for different temperatures. The spin susceptibility obtained by cGGW and GGW-RPA both satisfy the constrain of the SU(2), while the covariant GW (cGW) results violate this basic spin symmetry. Thus, we cannot point out which susceptibility from cGW is the static antiferromagnetic susceptibility clearly, and the calculation is nonsense.

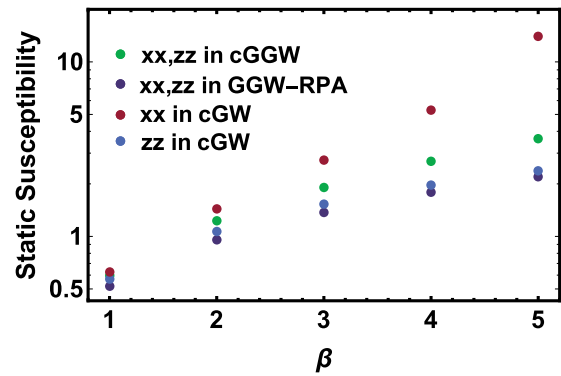


FIG. 5. The different components of the static antiferromagnetic spin susceptibility χ_{sp}^{xx} , χ_{sp}^{yy} , χ_{sp}^{zz} obtained by cGGW, GGW-RPA and cGW. The cGW violates the symmetry $\chi_{sp}^{xx}(p) = \chi_{sp}^{yy}(p) = \chi_{sp}^{zz}(p)$.

- [1] P. Coleman, *Introduction to Many-Body Physics* (Cambridge University Press, Cambridge, 2015).
- [2] G. Baym and L. P. Kadanoff, *Phys. Rev.* **124**, 287 (1961).
- [3] The RPA approximation is merely self-consistent with the Hartree or the Hartree-Fock Green's function within the Baym-Kadanoff framework.
- [4] A. L. Kutepov, *J. Phys.: Condens. Matter* **27**, 315603 (2015).
- [5] K. Morita, H. Maebashi, and K. Miyake, *Physica B* **312-313**, 547 (2002).
- [6] R. Kubo, *Rep. Prog. Phys.* **29**, 255 (1966).
- [7] L. S. Ornstein and F. Zernicke, *Proc. Acad. Sci. Amsterdam* **17**, 793 (1914).
- [8] L. Peliti, *Statistical Mechanics in a Nutshell* (Princeton University Press, Princeton, NJ, 2011).
- [9] A. Kovner and B. Rosenstein, *Phys. Rev. D* **39**, 2332 (1989).
- [10] B. Rosenstein and A. Kovner, *Phys. Rev. D* **40**, 504 (1989).
- [11] J. Wang, D. Li, H. Kao, and B. Rosenstein, *Ann. Phys.* **380**, 228 (2017).
- [12] L. Hedin, *Phys. Rev.* **139**, A796 (1965).
- [13] G. Onida, L. Reining, and A. Rubio, *Rev. Mod. Phys.* **74**, 601 (2002).
- [14] F. Aryasetiawan and O. Gunnarsson, *Rep. Prog. Phys.* **61**, 237 (1998).
- [15] F. Aryasetiawan and S. Biermann, *Phys. Rev. Lett.* **100**, 116402 (2008).
- [16] F. Aryasetiawan and S. Biermann, *J. Phys.: Condens. Matter* **21**, 064232 (2009).
- [17] X. Leng, F. Jin, M. Wei, and Y. Ma, *WIREs Comp. Mole. Sci.* **6**, 532 (2016).
- [18] L. Reining, *WIREs Comp. Mole. Sci.* **8**, e1344 (2018).
- [19] D. Golze, M. Dvorak, and P. Rinke, *Frontiers Chem.* **7**, 377 (2019).
- [20] A. Altland and B. D. Simons, *Condensed Matter Field Theory*, 2nd ed. (Cambridge University Press, Cambridge, 2010).
- [21] A. Larkin and A. Varlamov, *Theory of Fluctuations in Superconductors* (Oxford University Press, Oxford, 2005).
- [22] B. Rosenstein, M. Lewkowicz, and T. Maniv, *Phys. Rev. Lett.* **110**, 066602 (2013).
- [23] J. Smit, *Introduction to Quantum Fields on a Lattice*, Cambridge Lecture Notes in Physics (Cambridge University Press, Cambridge, 2002).
- [24] T. Schäfer and A. Toschi, *J. Phys.: Condens. Matter* **33**, 214001 (2021).
- [25] J. W. Negele and H. Orland, *Quantum Many-Particle Systems*, 1st ed. (CRC Press, Boca Raton, FL, 1998).
- [26] R. Blankenbecler, D. J. Scalapino, and R. L. Sugar, *Phys. Rev. D* **24**, 2278 (1981).
- [27] J. E. Hirsch, *Phys. Rev. B* **31**, 4403 (1985).
- [28] R. R. d. Santos, *Braz. J. Phys.* **33**, 36 (2003).
- [29] T. Schäfer, N. Wentzell, F. Šimkovic, Y.-Y. He, C. Hille, M. Klett, C. J. Eckhardt, B. Arzhang, V. Harkov, F. M. Le Régent, A. Kirsch, Y. Wang, A. J. Kim, E. Kozik, E. A. Stepanov, A. Kauch, S. Andergassen, P. Hansmann, D. Rohe, Y. M. Vilk, J. P. F. LeBlanc, S. Zhang, A. M. S. Tremblay, M. Ferrero, O. Parcollet, and A. Georges, *Phys. Rev. X* **11**, 011058 (2021).